Pergamon

SCIENCE DIRECT®

Tetrahedron Letters 44 (2003) 7277–7280

TETRAHEDRON LETTERS

A new class of azobenzene chelators for Mg^{2+} and Ca^{2+} in buffer at physiological pH

Atsuya Momotake and Tatsuo Arai*

University of Tsukuba, Tennnodai 1-1-1, Tsukuba 305-8571, Japan

Received 11 July 2003; revised 25 July 2003; accepted 1 August 2003

Abstract—A new class of azobenzene-based chelators, *trans*-**3a** and *trans*-**3b** (**3a** and **3b**), were designed and synthesized in two steps. Both **3a** and **3b** were readily dissolved in a buffer solution at physiological pH. The values of the dissociation constant of **3a** and **3b** for Mg^{2+} and Ca^{2+} were determined by the Hills plot; $K_d^{Mg}=1.12$ mM and $K_d^{Ca}=660$ μM for **3a** and $K_d^{Mg}=158$ μM and $K_d^{Ca}=200$ μM for **3b**, respectively. On irradiation at 489 nm light, **3a** isomerized to give *cis*-form, which underwent *cis*-to-*trans* thermal isomerization in darkness at room temperature. The change in the absorption spectrum of the irradiated solution of **3a** in the presence of Mg^{2+}, showing the *cis*-to-*trans* thermal isomerization, indicates that the affinity of *cis*-**3a** for Mg^{2+} is lower than that of **3a**.

Azobenzene and its analogues play an important role for a tremendous amount of functionalized molecules due to its efficient photo *trans*-*cis* and thermal *cis*-to-*trans* isomerization properties. In addition, many of the spectrophotometric reagents for detection of a metal ion in aqueous solution contain azobenzene skeletons.[1–3] Azobenzenes are key molecules for creating new functionalized molecules because (1) they are potential good chromophore and (2) they possess photo- and thermal-switchable properties. In this context basic studies of their photochemical behavior and of the structure–spectral relationship are essential for development of a new class of functionalized azobenzene derivatives. As a part of our research, we previously reported azobenzene dendrimers where the azobenzene works as a dendrimer core, to investigate the effect of a bulky dendron subunit on the isomerization properties.[4] In this study we focus our attention on the azobenzene as a potential good chromophore to develop photofunctionalized molecules such as caged calcium controlled by light.[5–7] We describe here the design, synthesis, photochemistry and binding properties of biologically important metals of a new class of water-soluble azobenzene chelators. The effect of methyl groups in the azobenzene ring on the binding and photochemical behavior is also incorporated.

For designing the azobenzene chelators, the following points were considered: (1) Absorption properties: If a chelator absorbs visible light, it could be a potential color indicator. In order to obtain an azobenzene derivative with large extinction coefficient at longer wavelength, electronic push–pull effect on the aromatic

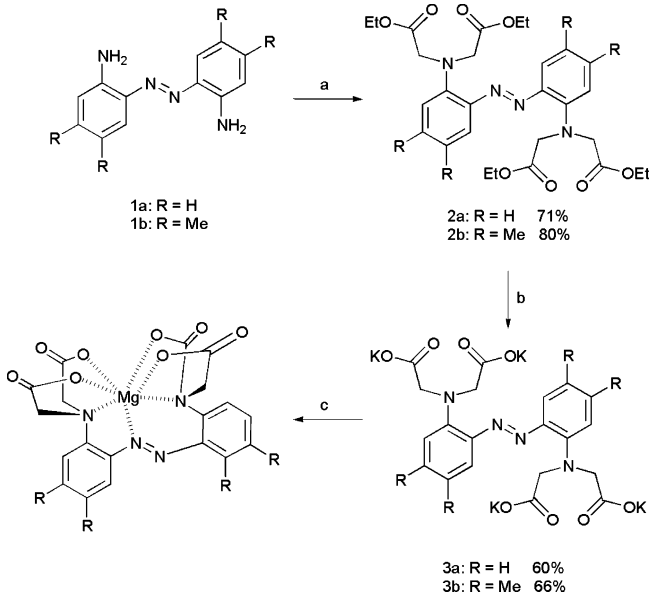

Scheme 1. *Reagents and conditions*: (a) Bromoethyl acetate, NaI, $(i\text{-Pr})_2NEt$, CH_3CN, reflux, 3–5 days; (b) KOH, EtOH, 12 h; (c) $MgCl_2$, HEPES, KCl buffer, pH 7.2, 22°C.

* Corresponding author. Tel.: +81-298-53-4315; fax: +81-298-53-6503; e-mail: arai@chem.tsukuba.ac.jp

0040-4039/$ - see front matter © 2003 Elsevier Ltd. All rights reserved.
doi:10.1016/S0040-4039(03)01863-X

ring will be helpful so that an electron-donating group should be introduced in the *ortho*- or *para*-position to the azo linkage; (2) Solubility: Water-solubility at physiological pH is necessary for chelating reagents if the targets are physiologically important metals, such as calcium and magnesium. In some cases, the binding constants for Ca^{2+} or Mg^{2+} are determined in an organic solvent[8] or a mixture of water–organic solvent probably because of the poor water-solubility of chelators.[9] Generally, the binding affinity is strongly affected by the solvent polarity, temperature, pH, and so forth. Therefore, before preparation, it should be considered that the chelators which are not water-soluble are hardly any help to measure the amount of the metals in aqueous solution; (3) Binding properties: Actually, it is difficult to estimate the binding affinity of the chelators for each metal before they are prepared. As the first series of compounds for this study, we chose the EDTA-like structures *trans*-**3a** and *trans*-**3b** (**3a** and **3b**) because it would increase not only the binding affinity for Ca^{2+} and Mg^{2+} but also water solubility as well as the electron-donating effect on the aromatic ring.

The chelator **3a** and its methyl derivative **3b** were obtained in two steps (Scheme 1), starting from **1a**[10] and **1b**[11] which were prepared by KO_2 oxidation of *o*-phenylenediamine for **1a** and of 4,5-dimethyl-1,2-phenylenediamine for **1b**, respectively. Alkylation of **1a** and **1b** with ethyl bromoacetate was achieved in refluxing acetonitrile in the presence of *N*,*N*-diisopropylethylamine and sodium iodide to give tetraalkylated azobenzene **2a** and **2b**, respectively, in moderate yield. Compounds **2a** and **2b** were saponified in aqueous KOH–ethanol. After the hydrolysis completed, the solvent was removed by evaporation and the crude product was dissolved in hot ethanol and diethyl ether was added. The mixture was allowed to stand for 30 min at room temperature to give a reddish-orange precipitate, which was an almost pure product. The obtained potassium salts **3a** and **3b** were characterized by UV, NMR and elemental analysis. Both compounds readily dissolved in water at physiological pH to give the red solution. The all products obtained in this procedure were *trans*-isomer, which were determined by ^{1}H NMR. *cis*-Isomers were not obtained probably because they were unstable to go back to corresponding *trans*-isomers at room temperature. The structure of Mg^{2+}-bound form of **3a** shown in Scheme 1 is tentative.

UV absorption spectra of **3a** and **3b** at various levels of free Mg^{2+} were monitored at room temperature as shown in Figure 1. In the absence of divalent ions, the spectrum shows a maximum at 489 and 316 nm for **3a** and 505 and 334 nm for **3b**, respectively in a buffer solution (40 mM Hepes/100 mM KCl, pH 7.2 at 22°C). The absorption maximum of **3b** slightly red-shifted by the effect of introduction of methyl groups in the *para*-position of azo-linkage. To the solution of the free chelator, increasing amounts of the $MgCl_2$ solution were added and after each titration step, absorption spectra were recorded. Magnesium ion binding to the chelator causes a major hypsochromic shift toward a limiting spectrum with a maximum at 473 and 322 nm

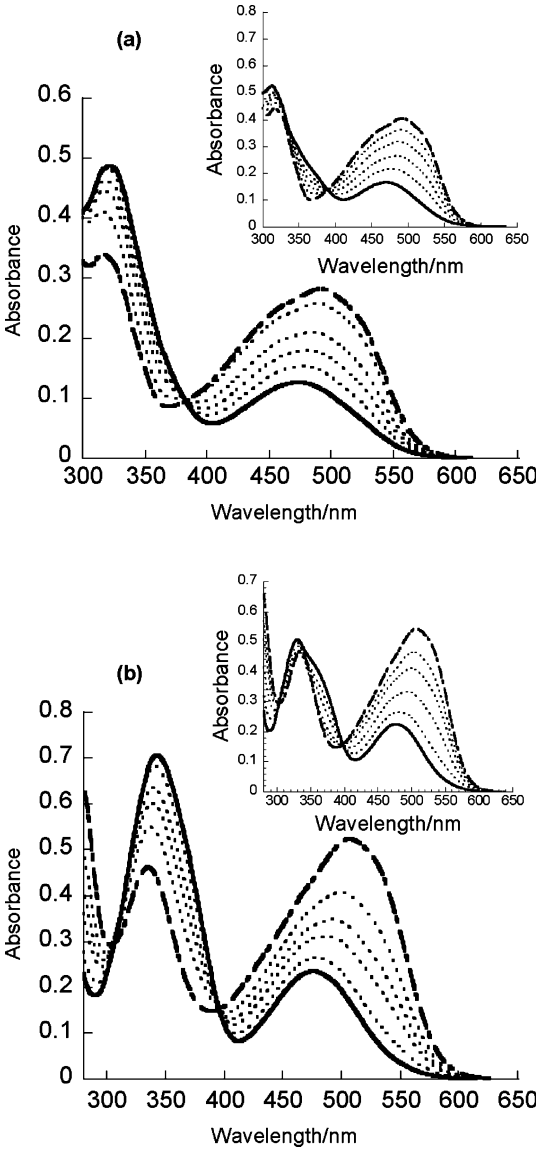

Figure 1. Change in absorption spectra of **3a** (a) and **3b** (b) upon the addition of $MgCl_2$ in 40 mM HEPES, 100 mM KCl buffer, pH 7.2, 22°C: before titration (dash-dot line) and excess $MgCl_2$ (solid line). Inset shows the similar spectral change upon the addition of $CaCl_2$.

for **3a** and 475 and 343 nm for **3b**, respectively. A series of spectra were conveniently analyzed by the Hill plot, i.e. a plot of $\log[(A-A_0)/(A_1-A)]=y$ versus $\log[Mg^{2+}]=x$. A_0 is the absorbance of the free tetraanion before titration, A_1 is the absorbance of the magnesium complex and A is the absorbance at intermediate magnesium level. The data were fit to a straight line and the value for K_d^{Mg} could be determined: 1.12 mM for **3a** and 158 μM for **3b**, respectively. The K_d^{Mg} value for **3b** is approximately seven times lower than that of **3a** suggesting that the binding affinity for Mg^{2+} is affected by the change in the electronic environment on the azobenzene aromatic ring due to the two methyl groups. The dissociation constant for Mg^{2+} found for **3a** in vitro is similar to the values reported for APTRA (aminophenol triacetic acid)-based magnesium chela-

tors.[12,13] Since the values correspond well with the low and submillimolar levels of cytosolic free Mg^{2+}, the chelators **3a** and **3b** may be used as the non-fluorescent colorimetric reagents for Mg^{2+} under physiological conditions. The dissociation constants for Ca^{2+} were also determined by the same method and were 660 and 200 μM for **3a** and **3b**, respectively. Similar spectral changes of **3a** and **3b** upon the addition of $CaCl_2$ are shown in the inset of Figure 1. It should be noted that **3a** and **3b** have higher selectivity for Mg^{2+} than for Ca^{2+} in intracellular fluid because the basal cellular free Ca^{2+} level, about 100 nM, is much lower than that of Mg^{2+}. This indicates that Ca^{2+} does not interfere with Mg^{2+} measurement under normal conditions in intracellular fluid.

Since compounds **3a** and **3b** are azobenzene analogues, photoisomerization was tested (Scheme 2). On irradiation at 489 nm light, the absorbance at 489 nm of **3a** decreased with time. Figure 2 shows the change in the absorption spectra of **3a**. Similar spectral change was observed on irradiation at 365 nm light. The ratio of **3a** and *cis*-**3a** at the photo-stationary state was $([trans]/[cis])_{pss} = 80/20$, determined by ^1H NMR. When the irradiated solution of **3a** was kept in darkness at room temperature, the absorbance at 489 nm increased and was mostly back to that of **3a** after 3 h with the rate constant of 1.43×10^{-2} s^{-1} at 22°C. These spectral changes with photoirradiation as well as dark reaction

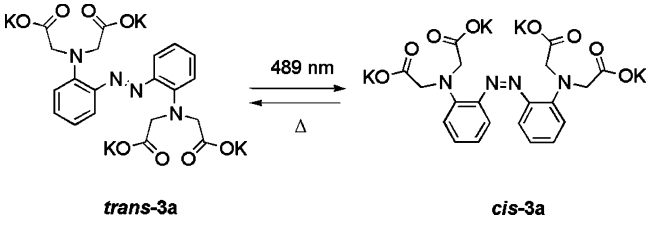

Scheme 2. Photo *trans–cis* and thermal *cis*-to-*trans* isomerization of **3a**.

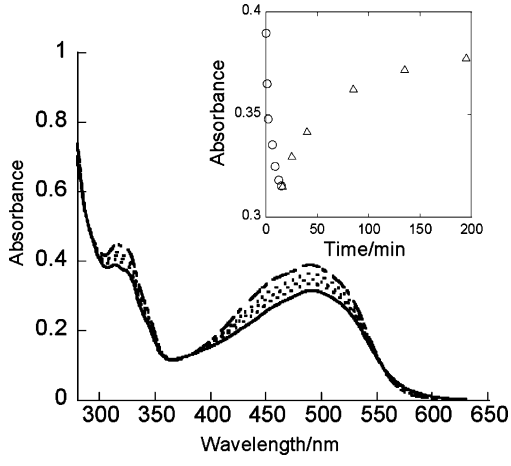

Figure 2. Change in absorption spectrum of *trans*-**3a** on irradiation at 489 nm in HEPES, KCl buffer, pH 7.2, 22°C. Inset shows the time dependence of the absorption change at 489 nm for photo *trans–cis* isomerization (○) and thermal *cis*-to-*trans* isomerization in the dark at 23°C (△).

are characteristic of *trans–cis* isomerization of an azobenzene chromophore. The inset in Figure 3 shows the time profile of photo *trans–cis* isomerization (○) on irradiation at 489 nm light and thermal *cis*-to-*trans* isomerization (△) of **3a** at 23°C in darkness. Methyl derivatives **3b**, on the other hand, did not isomerize on irradiation at 510 or 365 nm light in a buffer at pH 7.2. The present finding indicates that the introduction of electron-donating groups in the *para*-position of azo-linkage, in addition to the *ortho*-amino groups, probably increases the intramolecular charge transfer and affects the singlet excited state behavior, to result in change of the photoisomerization properties. Ca^{2+}- or Mg^{2+}-bound form of **3a** after titration also did not exhibit photoisomerization on irradiation at 489 or 365 nm light.

The difference in affinities of **3a** and *cis*-**3a** for Mg^{2+} was investigated. Figure 3 shows the change in the absorption spectra of **3a**. The absorbance of **3a**, 5.32×10^{-5} M in HEPES, KCl buffer, pH 7.2, 22°C (dotted line) decreased with irradiation at 489 nm light to give the *trans–cis* photostationary state (line not shown). Then, the absorbance of the irradiated solution was further decreased by addition of $MgCl_2$ (3.32×10^{-5} M) (thin line). Interestingly, the absorbance, observed just after adding $MgCl_2$, increased with time. When 160 min passed after addition of $MgCl_2$, the increasing spectra (○) overlapped with another spectrum of **3a** in the

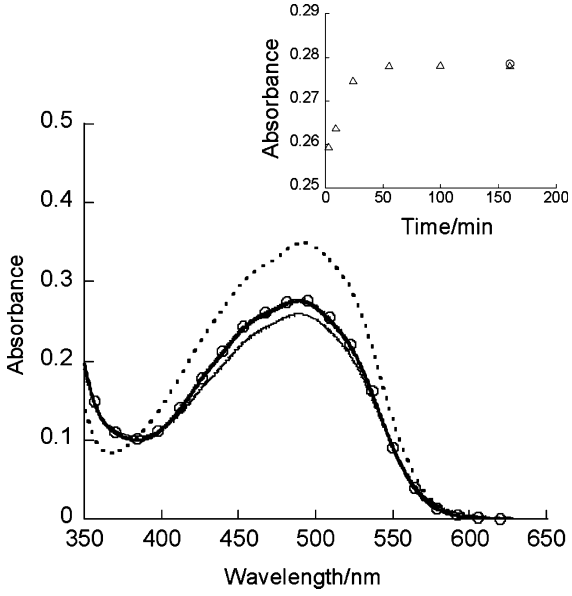

Figure 3. Absorption spectra of **3a** before irradiation in HEPES, KCl buffer, pH 7.2, 22°C (dotted line), after addition of $MgCl_2$ (3.32×10^{-5} M) without irradiation (solid line), right after addition of $MgCl_2$ (3.32×10^{-5} M) to the irradiated solution (thin line), and 160 min later after addition of $MgCl_2$ to the irradiated solution (○). Inset shows the time dependence of the absorbance change for irradiated solution of **3a** with added $MgCl_2$ (3.32×10^{-5} M), recorded at 489 nm for thermal *cis*-to-*trans* isomerization in the dark at 22°C (△) and absorbance of non-irradiated **3a** solution with added $MgCl_2$ (3.32×10^{-5} M) (○).

presence of $MgCl_2$ (3.32×10^{-5} M) (solid line). The result indicates that the affinity of the *cis*-isomer for Mg^{2+} is much lower than that of the *trans*-isomer (Scheme 3). The inset in Figure 3 shows the increase of the absorbance for the irradiated solution of **3a** with $MgCl_2$ (3.32×10^{-5} M), recorded at 489 nm, exhibiting the thermal *cis*-to-*trans* isomerization (△) and the absorbance of non-irradiated **3a** with $MgCl_2$ (3.32×10^{-5} M) (○).

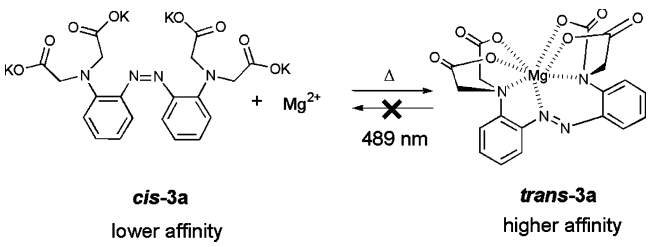

Scheme 3.

In summary, a new class of azobenzene-based chelators **3a** and **3b** was designed and synthesized by simple reactions and their basic properties were described. Both **3a** and **3b** were readily dissolved in water at physiological pH. Introduction of methyl groups in the aromatic ring affected the dissociation constant for metals as well as the photoisomerization properties. On irradiation at 489 nm light, **3a** isomerized to give *cis*-form, which underwent *cis*-to-*trans* thermal isomerization in darkness at room temperature. The experimental results on the absorption spectra of the irradiated solution of **3a** with Mg^{2+} indicate that the affinity of *cis*-**3a** for Mg^{2+} is much lower than that of **3a**. To the best of our knowledge, this is the first clear example to prepare photoresponsive azobenzene chelators where the affinity for Mg^{2+} is different between the *trans*- and *cis*-isomers. In addition, **3a** and **3b** can be used as a magnesium indicator under physiological conditions.

2a: ^{1}H NMR (400 MHz; $CDCl_3$; Me_4Si) δ 7.23 (2H, ddd, $J=8.1$, 7.0 and 1.8 Hz, ArH), 7.18 (2H, dd, $J=1.7$ and 8.1 Hz, ArH), 6.84–6.78 (4H, m, ArH), 4.26 (8H, s, NCH_2), 4.03 (8H, q, $J=7.1$ Hz, CH_2CH_3), 1.13 (12H, t, $J=7.1$ Hz, CH_3). ESI-MS: calcd for $C_{28}H_{34}N_4NaO_8$: $[M+Na]^+$; m/z 579.2431. Found: 579.2531. **2b**: ^{1}H NMR (400 MHz; $CDCl_3$; Me_4Si) δ 7.01 (2H, s, ArH), 6.57 (2H, s, ArH), 4.24 (8H, s, NCH_2), 4.07 (8H, q, $J=7.1$ Hz, CH_2CH_3), 2.21 (6H, s, CH_3), 2.15 (6H, s, CH_3), 1.13 (12H, t, $J=7.1$ Hz, CH_3). ESI-MS: calcd for $C_{32}H_{44}N_4NaO_8$: $[M+Na]^+$; m/z 635.3051. Found: 635.2949. **3a**: ^{1}H NMR (400 MHz; D_2O) δ 7.56 (2H, d, $J=7.7$ Hz, ArH), 7.30 (2H, t, $J=7.7$ Hz, ArH), 6.88–6.82 (4H, m, ArH), 4.06 (8H, s, NCH_2). Anal. calcd for $C_{20}H_{16}K_4N_4O_8\cdot9H_2O\cdot KOH$: C, 29.47; H, 4.33; N, 6.87. Found: C, 29.54; H, 4.11; N, 6.74. **3b**: ^{1}H NMR (400 MHz; D_2O) δ 7.41 (2H, s, ArH), 6.68 (2H, s, ArH), 4.40 (8H, s, NCH_2), 2.25 (6H, s, CH_3), 2.20 (6H, s, CH_3). Anal. calcd for $C_{24}H_{24}K_4N_4O_8\cdot9H_2O$: C, 35.37; H, 5.19; N, 6.87. Found: C, 35.59; H, 5.18; N, 6.82.

Acknowledgements

This work was supported by a Grant-in-Aid for Scientific Research on Priority Areas (417) and the 21 Century COE Program from the Ministry of Education, Culture, Sports, Science and Technology (MEXT) of the Japanese Government and by the Asahi Glass Foundation.

References

1. Ohshita, R.; Wada, H.; Nakagawa, G. *Anal. Chim. Acta* **1981**, *124*, 193–200.
2. Shibata, S. *Anal. Chim. Acta* **1960**, *23*, 367–369.
3. Horiguchi, D.; Saito, M.; Iwamura, T.; Kina, K. *Anal. Chem. Acta* **1983**, *151*, 457–463.
4. Uda, M.; Momotake, A.; Arai, T. *Photochem. Photobiol. Sci.* **2003**, *2*, 845–847.
5. Ellis-Davies, G. C. R.; Kaplan, J. H. *Proc. Natl. Acad. Sci.* **1988**, *85*, 6571–6575.
6. Ellis-Davies, G. C. R.; Kaplan, J. H. *Proc. Natl. Acad. Sci.* **1994**, *91*, 187–191.
7. Adams, S. R.; Kao, J. P. Y.; Grynkiewicz, G.; Minta, A.; Tsien, R. Y. *J. Am. Chem. Soc.* **1988**, *110*, 3212–3220.
8. Ajayaghosh, A.; Arunkumar, E.; Daub, J. *Angew. Chem., Int. Ed.* **2002**, *41*, 1766–1769.
9. Kim, E. J.; Choe, J.-I.; Chang, S.-K. *Tetrahedron Lett.* **2003**, *44*, 5299–5302.
10. Crank, G.; Makin, M. I. H. *Tetrahedron Lett.* **1979**, *23*, 2169–2170.
11. Crank, G.; Makin, M. I. H. *Aust. J. Chem.* **1984**, *37*, 845–855.
12. Otten, P. A.; London, R. E.; Levy, L. A. *Bioconjugate Chem.* **2001**, *12*, 76–83.
13. Cielen, E.; Stobiecka, A.; Tahri, A.; Hoornaert, G. J.; De Schryver, F. C.; Gallay, J.; Vincent, M.; Boens, N. *J. Chem. Soc., Perkin Trans. 2* **2002**, 1197–1206.